Furrow flexure and ancient heat flux on Ganymede

F. Nimmo
Department of Earth and Space Sciences, University of California, Los Angeles, California, USA

R. T. Pappalardo
Laboratory for Atmospheric and Space Physics, University of Colorado, Boulder, Colorado, USA

Received 16 June 2004; revised 12 August 2004; accepted 24 August 2004; published 2 October 2004.

[1] Stereo-derived topographic profiles across furrows in the ancient (~4 Gyr) dark terrain of Galileo Regio, Ganymede, suggest flexural uplift. Modeling of the rift-flank profiles implies an effective elastic thickness of ≈0.5 km, heat fluxes in the range 60–80 mW m^{-2} at the time of deformation, and a brittle-ductile transition depth of 2–3 km. The elastic thicknesses are comparable to estimates for grooved terrain on Ganymede, and chaos regions on Europa, and may be characteristic of the point during cooling at which the available stresses can no longer cause significant ice shell deformation. The furrowed dark terrain heat fluxes exceed likely chondritic values, and are plausibly a result of early cooling of Ganymede following accretion. Non-synchronous rotation may have contributed to the 2–3 MPa stresses required to cause the observed deformation. *INDEX TERMS:* 5418 Planetology: Solid Surface Planets: Heat flow; 5455 Planetology: Solid Surface Planets: Origin and evolution; 5475 Planetology: Solid Surface Planets: Tectonics (8149); 6218 Planetology: Solar System Objects: Jovian satellites; 8149 Tectonophysics: Planetary tectonics (5475). **Citation:** Nimmo, F., and R. T. Pappalardo (2004), Furrow flexure and ancient heat flux on Ganymede, *Geophys. Res. Lett.*, *31*, L19701, doi:10.1029/2004GL020763.

1. Introduction

[2] Ganymede's bimodal surface consists of bright and dark terrains which record a history of tectonic deformation. Dark terrain covers 1/3 of the surface and has a nominal crater age of >4 Gyr [*Zahnle et al.*, 2003]. The dark material itself is probably a lag of cometary and asteroidal refractory debris [*Prockter et al.*, 1998, 2000]. Dark terrain is cut by furrows, tectonic troughs that occur in sets of subconcentric or subradial structures and are typically 6 to 20 km wide [*Shoemaker et al.*, 1982]. The generally accepted explanation for furrows is that they are graben formed in response to ancient giant impacts soon after solidification of Ganymede's shell [*McKinnon and Melosh*, 1980]. Younger, bright grooved terrain is characterized by crosscutting sets of subparallel ridges and troughs, probably predominantly extensional in origin [*Shoemaker et al.*, 1982; *Pappalardo et al.*, 1998, 2004], and based on crater densities is nominally 2 Gyr old [*Zahnle et al.*, 2003].

[3] Using topographic data derived from stereo images obtained during the Galileo spacecraft's G28 orbit, *Nimmo et al.* [2002] inferred flexural flank uplift at two areas (Harpagia Sulcus and Arbela Sulcus) which underwent rifting during grooved terrain formation. These authors applied a flexural model to topographic profiles and derived a heat flux of ~100 mW m^{-2}. In this paper we carry out an analysis similar to [*Nimmo et al.*, 2002], to obtain effective elastic thickness and heat flux estimates in dark terrain. We further suggest possible scenarios for the evolution of Ganymede's heat flux with time.

0094-8276/04/2004GL020763$05.00

2. Data and Analysis

[4] A small portion of Galileo Regio (~6400 km^2) was imaged in stereo during the Galileo spacecraft's G1 and G2 encounters with Ganymede (Figure 1). A digital elevation model (DEM) has been derived using autocorrelation techniques from 3 × 3 pixel averaging of these stereo images, resulting in topographic horizontal resolution of 500 to 1000 m (nominally 600 m) and vertical resolution of 20 to 40 m. The DEM is described in detail by *Giese et al.* [1998], and has been used previously by *Prockter et al.* [1998].

[5] *Prockter et al.* [1998] performed geological mapping of the G1/G2 Galileo Regio target area, including its furrows and inferred faults (Figure 1a). The NW-SE trending furrows of the Lakhmu Fossae system are morphologically subdued and associated with many individual obliquely trending fault scarps. The Lakhmu structures are transected by a more distinct and narrow (~10 km wide) N-S trending furrow of the Zu Fossae system; no tectonic features later than the Zu system are observed. Both furrows show the topographic signature expected of flexural rift-flank uplift (Figure 1b). The Zu structures clearly post-date the Lakhmu structures, and generally show slightly greater topographic relief.

[6] Following methods identical to *Nimmo et al.* [2002], we extracted topographic profiles from the Galileo Regio DEM, stacked these profiles to reduce topographic "noise," and then modeled the stacked profiles using an elastic flexure model. Profiles were obtained approximately perpendicular to the trends of the Zu (A–I) and Lakhmu (J–Q) Fossae, while avoiding data gaps and impact craters (Figure 1a). We also extracted profiles (R–U) across a portion of a furrow rim in the SW corner of the DEM, which is also part of the Lakhmu Fossae system.

[7] Prior to stacking, each profile was interpolated to a uniform point spacing of 0.3 km and the mean elevation subtracted. Stacking was accomplished by aligning the profiles so that the top of each fault scarp coincided, to isolate that scarp and any associated flank uplift. Figure 2a plots portions of the stacked profiles, together with dashed lines denoting ± one standard deviation.

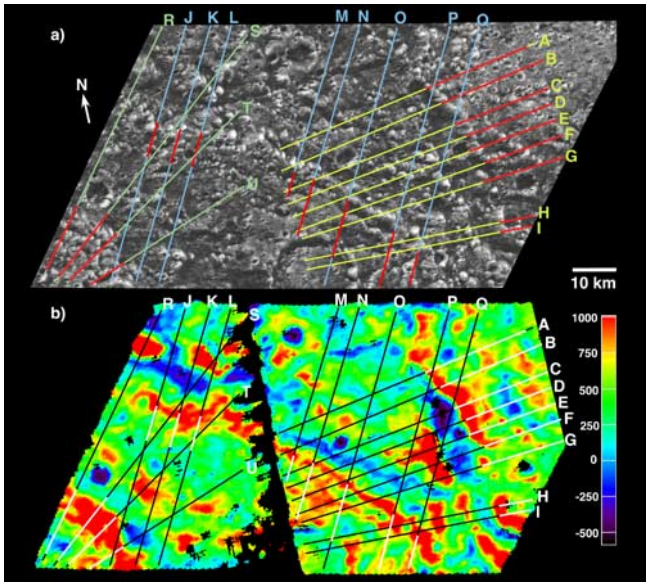

Figure 1. a) High-resolution image (80 m/pixel) of Galileo Regio, centered at approx. 18° lat., 149° long. (see *Prockter et al.* [1998] for details). Shown here are the full profiles extracted from the DEM (Zu profiles are yellow; Lahkmu profiles are blue; SW Lakhmu furrow profiles are green). Subsections of these profiles were stacked for analysis, and red indicates the segment sections which were fit following stacking (see Figure 2). b) Stereo topography from images s0359944739 and s0349759052 (see *Giese et al.* [1998] for details). Horizontal resolution ≈600 m, vertical resolution 20–40 m. Here the full profiles are black, and the fit segments are white.

[8] We modeled the flexural profile of a broken elastic plate, appropriate if the rift-zone bounding fault has penetrated the elastic layer, using the technique of *Barnett et al.* [2002]. The horizontal length-scale of the plate deflection depends on the flexural parameter α, where

$$\alpha = \left[\frac{ET_e^3}{3(1-\nu^2)\rho g}\right]^{1/4}. \quad (1)$$

Here T_e is the effective elastic thickness of the plate, E is the Young's modulus, ν is Poisson's ratio, g is the acceleration due to gravity, and ρ is the density of the fluid or viscous substratum.

[9] Using the method of *Barnett et al.* [2002] we varied T_e to minimize the misfit between the model and the topographic observations. Profiles having a misfit greater than 1.3 times the minimum value produced a visibly poorer fit, so this criterion was adopted to infer the acceptable range of T_e values.

[10] Equation (1) shows that the results are only weakly dependent on Young's modulus. Here we use a value of 1 GPa, based on terrestrial tidal flexure modelling [*Vaughan*, 1995]; uncertainties in this value do not affect the results significantly. We adopt a Poisson's ratio of 0.33, a density of 1000 kg m^{-3}, gravity of 1.43 m s^{-2} and a surface temperature of 120 K.

[11] The value of T_e obtained is the lowest since the time of loading [*Watts*, 2001]. This T_e value can be related to the heat flux using the yield-strength envelope technique [*McNutt*, 1984]. In this approach, the base of the lithosphere (that part of the ice shell which does not take part in convection) is specified by a particular stress level. Convective modelling suggests that the convecting interiors of ice shells are at 250–260 K [e.g., *Nimmo and Manga*, 2002]. We therefore define the base of the lithosphere as the 230 K isotherm, but the results are not very sensitive to reasonable variations in this quantity. The yield-stress envelope technique takes account of brittle, elastic and ductile deformation [see *Watts*, 2001, p. 276] and depends on the topographic curvature K, defined as the second derivative of the plate deflection. Higher curvatures, lower strain rates, or higher heat fluxes result in lower values of T_e.

[12] We adopt a thermal conductivity for ice that varies as $567/T$ [*Klinger*, 1980] and use the basal slip (n = 1.8) rheology of *Goldsby and Kohlstedt* [2001], with a nominal grain size of 1 mm. The coefficient of friction of cold ice is taken as 0.6 [*Beeman et al.*, 1988]. As discussed below, the results are not very sensitive to either rheology or strain rate; for the latter we adopt a nominal value of 10^{-15} s^{-1},

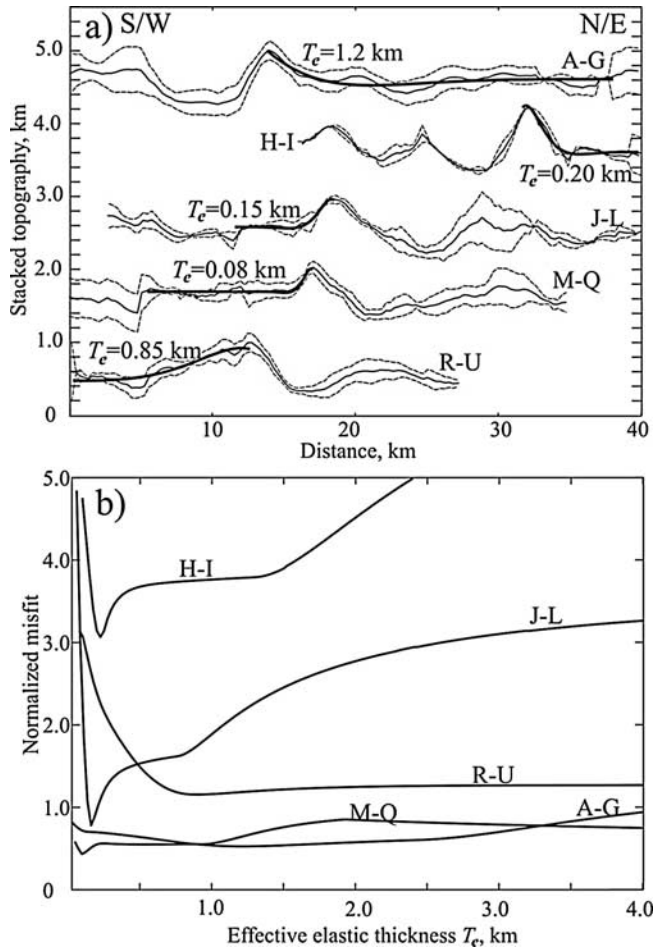

Figure 2. a) Portions of stacked profiles. Solid line is mean profile, thin lines are ± one standard deviation. Profiles A–I cross Zu, J–Q cross Lakhmu and R–U cross the SW Lakhmu furrow. Thick line is the best-fit theoretical profile (see text) with elastic thickness T_e as stated. Successive profiles are vertically offset by 1 km for clarity. b) Misfit as a function of T_e for each stacked profile.

Table 1. Results of Profile-Fitting[a]

Profile	T_e, km	K, m^{-1}	T_e Range, km	K Range, 10^{-4} m^{-1}	Min. Misfit	Misfit (0.5 km)	F, mW m^{-2}
A–G	1.20	3.7×10^{-5}	0.3–2.9	1.5–0.1	0.53	0.64	50 (31–132)
H–I	0.20	1.1×10^{-3}	0.1–1.6	23–0.5	3.08	3.69	100 (33–154)
J–L	0.15	1.0×10^{-3}	0.1–0.2	14–4.2	0.79	1.54	137 (135–184)
M–Q	0.08	2.0×10^{-3}	0–1.0	–0.4	0.44	0.56	205 (59–)
R–U	0.85	9.0×10^{-5}	0.4–	2.9–	1.17	1.41	53 (–77)
Har.	0.90	5.1×10^{-5}	0.1–1.1	12–0.4	1.30	1.31	60 (53–194)
Ar.	0.18	4.5×10^{-4}	0.1–0.9	8.4–0.5	0.54	0.62	154 (62–224)

[a]Har. and Ar. are results for Harpagia and Arbela Sulci, re-calculated from profiles in *Nimmo et al.* [2002]. K is the maximum curvature, T_e is elastic thickness. Ranges in T_e and K are for misfits $\leq$1.3 times the minimum value; note that max. T_e value implies min. K value. Penultimate column gives misfit for a fixed T_e of 0.5 km. F is the heat flux obtained using the best-fit T_e and the yield-strength envelope technique (see text). The range in brackets uses the max. and min. T_e values and the corresponding curvatures.

consistent with the results of *Dombard and McKinnon* [2001].

3. Results and Uncertainties

[13] Figure 2a shows the best-fit theoretical profiles obtained using the method outlined above, and Figure 2b shows the misfit as a function of T_e for each profile. In general, uncertainties in T_e are smallest when the matched profiles include a horizontal portion comparable to the flexural wavelength and the topography is not too rough (e.g., H–I, J–L). The lower bound on T_e is usually more tightly constrained than the upper bound (Figure 2b).

[14] Table 1 summarizes our results, and shows that with the exception of profiles J–L, all profiles can be fit to within the desired uncertainty by using T_e = 0.5 km. Figure 3 depicts these results, plotting the best-fit T_e and associated curvature values together with their upper and lower limits. As expected, K is inversely correlated with T_e. There appears to be no systematic difference between the Lakhmu and Zu furrows in terms of T_e or K.

[15] Also plotted are the values of T_e and K derived by *Nimmo et al.* [2002] for two sites of flexural uplift alongside the younger grooved terrain of Harpagia Sulcus and rifted terrain adjacent to Arbela Sulcus. The best-fit value for Arbela is smaller than that originally published (T_e = 1.7 km) because of an error caused by interpolation in the first 1.2 km of the original profile. Again, an acceptable fit to these profiles can be obtained using T_e = 0.5 km (Table 1).

[16] Included in Figure 3 are contours of heat flux (in mW m^{-2}) for a given T_e and curvature, based on the yield strength envelope technique described above. Table 1 shows that all the observations, except for profiles J–L, can be fit within the defined error by a heat flux in the range 60–80 mW m^{-2}. These results are consistent with the 30 to 120 mW m^{-2} derived from necking analysis of Ganymede rift zones by *Dombard and McKinnon* [2001]. *Nimmo et al.* [2002] obtained heat flux values of ~100 mW m^{-2} based on a T_e of ~1 km.

[17] The likely heat flux range of 60–80 mW m^{-2} applies to furrowed areas which have not been heavily deformed. Rifting in some areas of Ganymede generates stretching factors up to 100% [*Pappalardo and Collins*, 2004], which will cause local heat fluxes to exceed the background values by up to a factor of 2. Mass wasting, if significant, will result in longer topographic wavelengths and thus an overestimate of T_e and an underestimate in the heat fluxes.

[18] Because of the time elapsed since furrow formation, and the possibility of a heat pulse accompanying grooved terrain formation [*Nimmo et al.*, 2002], viscoelastic relaxation of the topography may have taken place [*Watts*, 2001]. Such relaxation would reduce the T_e measured at the present day, and thus lead to a potential overestimate of the heat flux at the time of deformation. Whether relaxation occurs depends on the viscosity of the ice, which is controlled by temperature and strain rate. Unless the strain rate is less than 10^{-19} s^{-1}, or 1% strain accumulation over 3 Gyr, near-surface ice will deform in a brittle fashion and will not relax. If the stresses in the ductile portion of the yield-strength envelope are set to zero (indicating complete relaxation), the result is a reduction in T_e of 10%–27% for strain rates of 10^{-15}–10^{-18} s^{-1}. It is therefore likely that relaxation is a relatively small effect; nonetheless, it would be valuable to carry out a more comprehensive study of this effect.

[19] Because the yield-strength envelope is dominated by the brittle portion, varying the strain rate or ice rheology has relatively little effect on the results. Varying the strain rate from 10^{-18} s^{-1} to 10^{-13} s^{-1} results in a change in T_e by 50% for the same heat flux. Varying the grain size from 0.1 mm to 10 mm results in a change in T_e of 20%. Using the n = 2.4 rheology of [*Goldsby and Kohlstedt*, 2001]

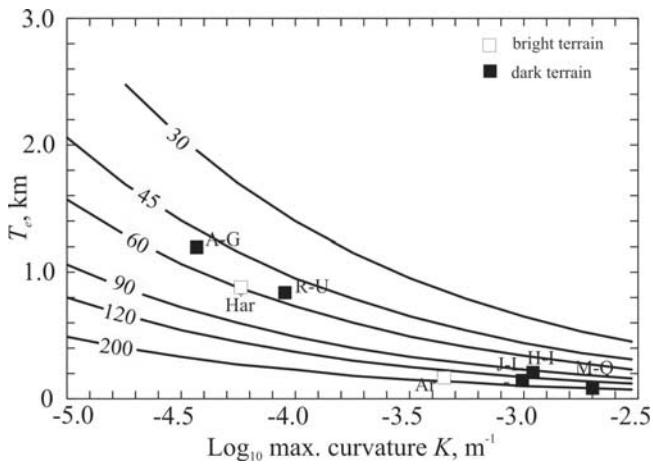

Figure 3. Elastic thickness T_e as a function of curvature K. Squares plot best-fit results from Table 1. Solid lines are theoretical T_e values using yield-strength envelope approach (see text) and assuming a strain rate of 10^{-15} s^{-1}; contour values are heat flux in mW m^{-2}. "Har" and "Ar" are Harpagia Sulcus and Arbela Sulcus results from Table 1.

results in a decrease in T_e of 20%. Finally, a reduction in the base lithosphere temperature to 200 K results in a decrease in inferred heat flux by ≈15%.

4. Discussion

[20] The heat flux through the ice shell is controlled by radiogenic heat production and cooling within the silicate interior, plus any tidal heating in the ice shell and/or silicate mantle. A heat flux of 60 to 80 mW m^{-2} exceeds the 40 mW m^{-2} that can be supplied by chondritic radioactive heating at 4.5 Gyr B.P. [*McKinnon and Parmentier*, 1986]. The conductive shell thickness implied by the heat flux values is 5–8 km, though if convection was operating, the shell thickness could have been much higher.

[21] The high heat flux recorded by the Galileo Regio furrows was probably caused by Ganymede's mantle cooling from initially high temperatures generated by accretion and (probably) differentiation. This conclusion is consistent with stratigraphic relationships, which suggest that furrows are among Ganymede's most ancient features, predating most large impact craters and palimpsests [*Shoemaker et al.*, 1982].

[22] Rapid mantle cooling can only explain the high heat fluxes inferred for the grooved terrain deformation if that deformation took place early, prior to about 4 Gyr B.P. This possibility cannot be excluded, owing to the uncertainty in crater calibration [*Zahnle et al.*, 2003]. However, other scenarios, such as a later passage through a Laplace-like resonance, seem more likely [*Showman and Malhotra*, 1997].

[23] Given the uncertainties, there is no evidence for heat fluxes at furrowed terrain being significantly different to grooved terrain sites. One possible explanation for this observation is that the older furrowed terrains were heated during the later grooved terrain deformation event, and pre-existing elastic thicknesses were re-set. If this is the case, or if relaxation is an important factor, then the furrowed terrain may contain no information about ancient heat fluxes on Ganymede. However, such re-heating seems unlikely, given that there is no clear evidence for later tectonic deformation of the Galileo Regio area [*Prockter et al.*, 2000]. More likely, the similar heat fluxes inferred for the two episodes of tectonism are characteristic of the point during cooling at which the ice shell became sufficiently strong that the available stresses could no longer cause deformation. If this hypothesis is correct, it may explain why T_e values similar to the ≈0.5 km obtained here are inferred for some regions of Europa [e.g., *Williams and Greeley*, 1998].

[24] The brittle-ductile transition depth implied by a heat flux of 60–80 mW m^{-2} is roughly 2–3 km, and implies stresses of 2–3 MPa are required to cause brittle deformation. Such stresses are too high to be generated by tidal forces, even during an episode of higher eccentricity [*Showman and Malhotra*, 1997]. However, non-synchronous rotation can develop MPa-level stresses [*Leith and McKinnon*, 1996], and cratering evidence suggests that such rotation has taken place on Ganymede [*Zahnle et al.*, 2003]. Thus, the early episode of deformation on Ganymede recorded by the furrows is plausibly a result of rapid initial cooling accompanied by non-synchronous rotation (NSR). Since both the cooling rate and the existence of NSR depend on the state of Ganymede's interior at that time, this scenario may allow constraints to be placed on Ganymede's early thermal evolution.

[25] **Acknowledgments.** We are very grateful to B. Giese for use of the Galileo Regio DEM, to C. Bader, L. DeRemer and A. Barr for invaluable assistance, and to L. Prockter, B. Banerdt and an anonymous referee for helpful comments. Support was provided by NASA PGG grants NAG5-11616 and NNG04GE89G, the NASA PGG Undergraduate Research Program, and the Royal Society.

References

Barnett, D. N., F. Nimmo, and D. McKenzie (2002), Flexure of Venusian lithosphere measured from residual topography and gravity, *J. Geophys. Res.*, *107*(E2), 5007, doi:10.1029/2000JE001398.

Beeman, M., W. B. Durham, and S. H. Kirby (1988), Friction of ice, *J. Geophys. Res.*, *93*, 7625–7633.

Dombard, A. J., and W. B. McKinnon (2001), Formation of grooved terrain on Ganymede: Extensional instability mediated by cold, superplastic creep, *Icarus*, *154*, 321–336.

Giese, B., J. Oberst, T. Roatsch, G. Neukum, J. W. Head, and R. T. Pappalardo (1998), The local topography of Uruk Sulcus and Galileo Regio obtained from stereo images, *Icarus*, *135*, 303–316.

Goldsby, D. L., and D. L. Kohlstedt (2001), Superplastic deformation of ice: Experimental observations, *J. Geophys. Res.*, *106*, 11,017–11,030.

Klinger, J. (1980), Influence of a phase transition of ice on the heat and mass balance of comets, *Science*, *209*, 271–272.

Leith, A. C., and W. B. McKinnon (1996), Is there evidence for polar wander on Europa?, *Icarus*, *120*, 387–398.

McKinnon, W. B., and H. J. Melosh (1980), Evolution of planetary lithospheres: Evidence from multiring basins on Ganymede and Callisto, *Icarus*, *44*, 454–471.

McKinnon, W. B., and E. M. Parmentier (1986), Ganymede and Callisto, in *Satellites*, edited by J. A. Burns and M. S. Matthews, pp. 718–763, Univ. of Ariz. Press, Tucson.

McNutt, M. K. (1984), Lithospheric flexure and thermal anomalies, *J. Geophys. Res.*, *89*, 11,180–11,194.

Nimmo, F., and M. Manga (2002), Causes, characteristics and consequences of convective diapirism on Europa, *Geophys. Res. Lett.*, *29*(23), 2109, doi:10.1029/2002GL015754.

Nimmo, F., R. T. Pappalardo, and B. Giese (2002), Effective elastic thickness and heat flux estimates on Ganymede, *Geophys. Res. Lett.*, *29*(7), 1158, doi:10.1029/2001GL013976.

Pappalardo, R. T., et al. (1998), Grooved terrain on Ganymede: First results from Galileo high-resolution imaging, *Icarus*, *135*, 276–302.

Pappalardo, R. T., and G. C. Collins (2004), Strained craters on Ganymede, *J. Struct. Geol.*, in press.

Pappalardo, R. T., G. C. Collins, J. W. Head, P. Helfenstein, T. McCord, J. M. Moore, L. M. Prockter, P. M. Schenk, and J. Spencer (2004), Ganymede, in *Jupiter: The Planet, Satellites and Magnetosphere*, edited by F. Bagenal et al., Univ. of Ariz. Press, Tucson, in press.

Prockter, L. M., et al. (1998), Dark terrain on Ganymede: Geological mapping and interpretation of Galileo Regio at high resolution, *Icarus*, *135*, 317–344.

Prockter, L. M., P. H. Figueredo, R. T. Pappalardo, J. W. Head, and G. C. Collins (2000), Geology and mapping of dark terrain on Ganymede and implications for grooved terrain formation, *J. Geophys. Res.*, *105*, 22,519–22,540.

Shoemaker, E. M., B. K. Lucchita, J. B. Plescia, S. W. Squyres, and D. E. Wilhelms (1982), The geology of Ganymede, in *Satellites of Jupiter*, edited by D. Morrison, pp. 435–520, Univ. of Ariz. Press, Tucson.

Showman, A. P., and R. Malhotra (1997), Tidal evolution into the Laplace resonance and the resurfacing of Ganymede, *Icarus*, *127*, 93–111.

Vaughan, D. G. (1995), Tidal flexure at ice shell margins, *J. Geophys. Res.*, *100*, 6213–6224.

Watts, A. B. (2001), *Isostasy and Flexure of the Lithosphere*, Cambridge Univ. Press, New York.

Williams, K. K., and R. Greeley (1998), Estimates of ice thickness in the Conamara Chaos region of Europa, *Geophys. Res. Lett.*, *25*, 4273–4276.

Zahnle, K., P. M. Schenk, H. F. Levison, and L. Dones (2003), Cratering rates in the outer solar system, *Icarus*, *163*, 263–289.

F. Nimmo, Department of Earth and Space Sciences, University of California, 595 Charles Young Drive E, Los Angeles, CA 90095-1567, USA. (nimmo@ess.ucla.edu)

R. T. Pappalardo, Laboratory for Atmospheric and Space Physics, University of Colorado, Campus Box 392, Boulder, CO 80309, USA. (robert.pappalardo@colorado.edu)